

Analysis of mechanical response of fistula plug for structure optimization

Shunli Yang,¹ Bin Jiang,² Feng Xu,^{1,3} Min Lin,¹ Guiping Zhao,^{1, a)} and Tianjian Lu^{1, b)}

¹⁾ Biomedical Engineering and Biomechanics Center, Xi'an Jiaotong University, Xi'an 710049, China

²⁾ NanJingHospital of T.C.M, Nanjing 210001, China

³⁾ The Key Laboratory of Biomedical Information Engineering of Ministry of Education, School of Life Science and Technology, Xi'an Jiaotong University, Xi'an 710049, China

(Received 08 November 2011; accepted 25 November 2011; published online 10 January 2012)

Abstract Anal fistula is one of the three greatest anorectal diseases with a high prevalence. The traditional treatments (e.g., surgery) for fistula have limitations due to damage to the internal anal sphincter of patients. With recent advances in biomaterials, treatments based on biomaterial filling (e.g., scleraprotein injection, fistula plug) have emerged as novel therapies for fistula. The anal fistula plug (e.g., based on small intestinal submucosa (SIS)) has attracted increasing attention because of short term healing rate and biocompatibility. However, challenges remain for this method such as plug falling as observed in clinics. To address this, this paper analyzes the case of SIS falling under physiological condition from mechanical point of view using ANSYS simulation. It then proposes three new geometrical structures for fistula plug and compares their mechanical behavior (e.g., axial stress, reaction of constraint) with that of clinically used structure (cone shape). Based on the simulation, it optimizes the geometric parameters of fistula plug. The approach developed here can help to improve the design of fistula plug for better clinical treatments. © 2012 The Chinese Society of Theoretical and Applied Mechanics. [doi:10.1063/2.1201407]

Keywords anal fistula, small intestinal submucosa, fistula plug, structure optimization, numerical simulation

Anal fistula is a tract connecting anal canal or rectum and perianal skin (Fig. 1(a)), which is usually induced by surgery. Traditionally, surgery is performed for treating fistula. However, traditional surgery may induce damage to anal sphincter and cause great pain, which negatively affects life quality of patients.¹ Therefore, more effective treatment are urgently needed for fistula.

With recent advances in biomaterials such as hydrogels,² there are widespread applications of biocompatible biomaterials in clinics including treatment of anal fistula.³ For instance, fistula plug made with small intestinal submucosa (SIS) is now used widely for fistula treatment⁴ (Fig. 1(b)). This treatment can protect patient's sphincter with reduced pain sensation and the patient may get back to work soon. Fistula plug is therefore strongly recommended by American Society of Colon and Rectal Surgeons (ASCRS).³ Fistula plug can also be combined with other traditional treatments to improve the cure rate.⁵ However, the failure of fistula plug (e.g., falling) often occurs. Although the reason for this failure has not been unified, it is generally accepted that the mechanical loading during sitting or running makes the plug falling.⁶⁻⁸ To prevent the plug falling, the plug has been designed as a cone shape⁴ and is fixed with surrounding tissues using suture during surgery (Fig. 1(b)). However, the falling rate remains high. There is still an unmet need to understand the falling mechanism and improve the plug structure.

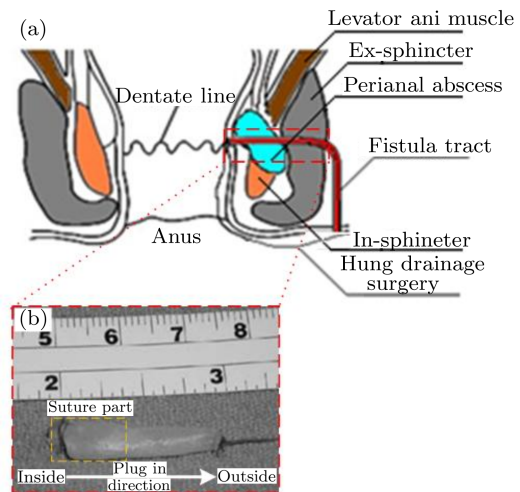


Fig. 1. Treatment of fistula using plug: (a) schematic of fistula; (b) its clinical treatment with fistula plug.⁴ The plug is dragged to fill the fistula in the direction from the inside of fistula tract.

In this study, we performed mechanical analysis of the fistula plug under physiological condition (i.e., under loading of body weight). We hypothesized that the falling off is due to the axial force applied on the plug by the surrounding tissues. To check this hypothesis, we performed a numerical simulation based on finite element method (FEM) using ANSYS.

According to the clinically relevant structure (Fig. 1(b)), we built a physical model for the fistula

^{a)} Corresponding author. Email: zhaogp@mail.xjtu.edu.cn.

^{b)} Email: tjlu@mail.xjtu.edu.cn.

Table 1. The geometry parameters of plug used in this study.

Total length	Suture length	Face diameter	Face diameter 2
\bar{L}_0	\bar{L}_1	\bar{D}_1	\bar{D}_2
1	0.13	0.22	0.13

plug (Fig. 2(a)). We chose the properties of SIS in this study (e.g., Young's modulus⁹), which is widely used in clinics for fistula plug due to its good biocompatibility. Although there is limited data reported in literature on the SIS's mechanical property, SIS has the hyperelastic mechanical property close to the rubber according to its uniaxial tensile stress-strain relationship.⁹ Besides, we observed in clinics that the SIS plug can return to its original shape when it falls off. Therefore, we assumed the poisson's ratio of SIS to be 0.5 and used Neo-Hookean model for SIS, which can use a stress-strain curves of one deformation to forecast other deformations.¹⁰ The material model is presented as

$$W = C_{01}(I_1 - 3)^2, \quad (1)$$

where W is the density of strain energy, C_{01} is equal to half of initial shear modulus and the I_1 is the first invariant of Green Strain. I_1 can be presented as

$$I_1 = \varepsilon_1 + \varepsilon_2 + \varepsilon_3, \quad (2)$$

where ε_1 , ε_2 , ε_3 are the first, second and third principal strain, respectively.

Initial shear modulus of 3.33 kPa was used in this study, which was obtained from the stress-strain data of SIS reported in literature.⁹ The geometry data of the plug used in this paper is from clinics and we used dimensionless scales based on the total length ($L_0 = 2.3$ cm) (Table 1).

$$\bar{L}_0 = L_0/L_0, \quad \bar{L}_1 = L_1/L_0, \\ \bar{D}_1 = D_1/L_0, \quad \bar{D}_2 = D_2/L_0,$$

where L_0 is the total length, and L_1 , D_1 , D_2 are the length of suture part, diameter 1 and diameter 2 of the plug, respectively.

Fistula plug is implanted into patient's fistula tract by surgery and fixed with surrounding tissues using surgery suture at the suture part (Fig. 2(b)). We set the mechanical boundary conditions and loading based on body weight (Fig. 2(c)). In the numerical model, an axial displacement constraint was set on surface at the suture part, where the plug is sutured to the surrounding tissues. The displacements in the radial direction and circumference direction on surface at the suture part are set free. The surface of other parts has no constraint. The pressure P_0 is the rectal resting pressure and P is the pressure caused by body weight. The P_0 was set as 2 200 kPa for a normal person¹¹ and P was estimated as half of body weight (70 kg) divided by the

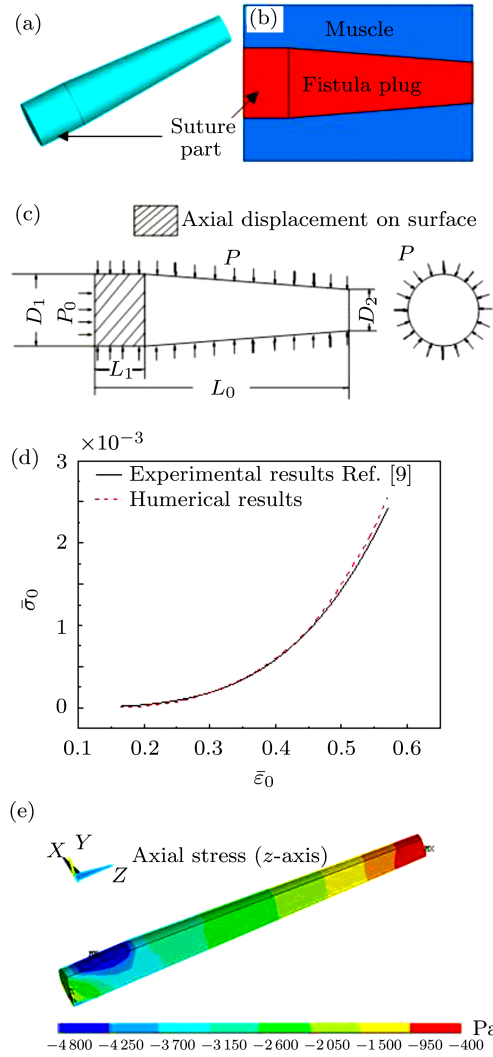


Fig. 2. Mechanical analysis of clinically used fistula plug: (a) the FEM model of plug; (b) the enlarged view of fistula; (c) schematic diagram of loading and displacement of plug; (d) verification of FE model, and (e) the axial stress of clinically used plug.

cross section area at waist. The reaction of constraint on the plug (e.g., suture part) will apply force to the surrounding tissues sutured to the plug. If this force is large, it may induce cell death and increase the falling possibility. With this physical model and mechanical loading, we first verified our numerical model with the experimental result from the literature⁹ (Fig. 2(d)). We observed good agreement between our simulation and experimental data. We then checked the axial stress of plug under body weight (Fig. 2(e)). It could be found from the results that the reaction of plug (axial stress on the surface of suture part) is large. For example, the axial stress on the surface of suture part is more than 2 times of pressure. This may be the reason for the high falling rate.

To decrease the reaction and address the problem of the plug falling, we proposed three new plug struc-

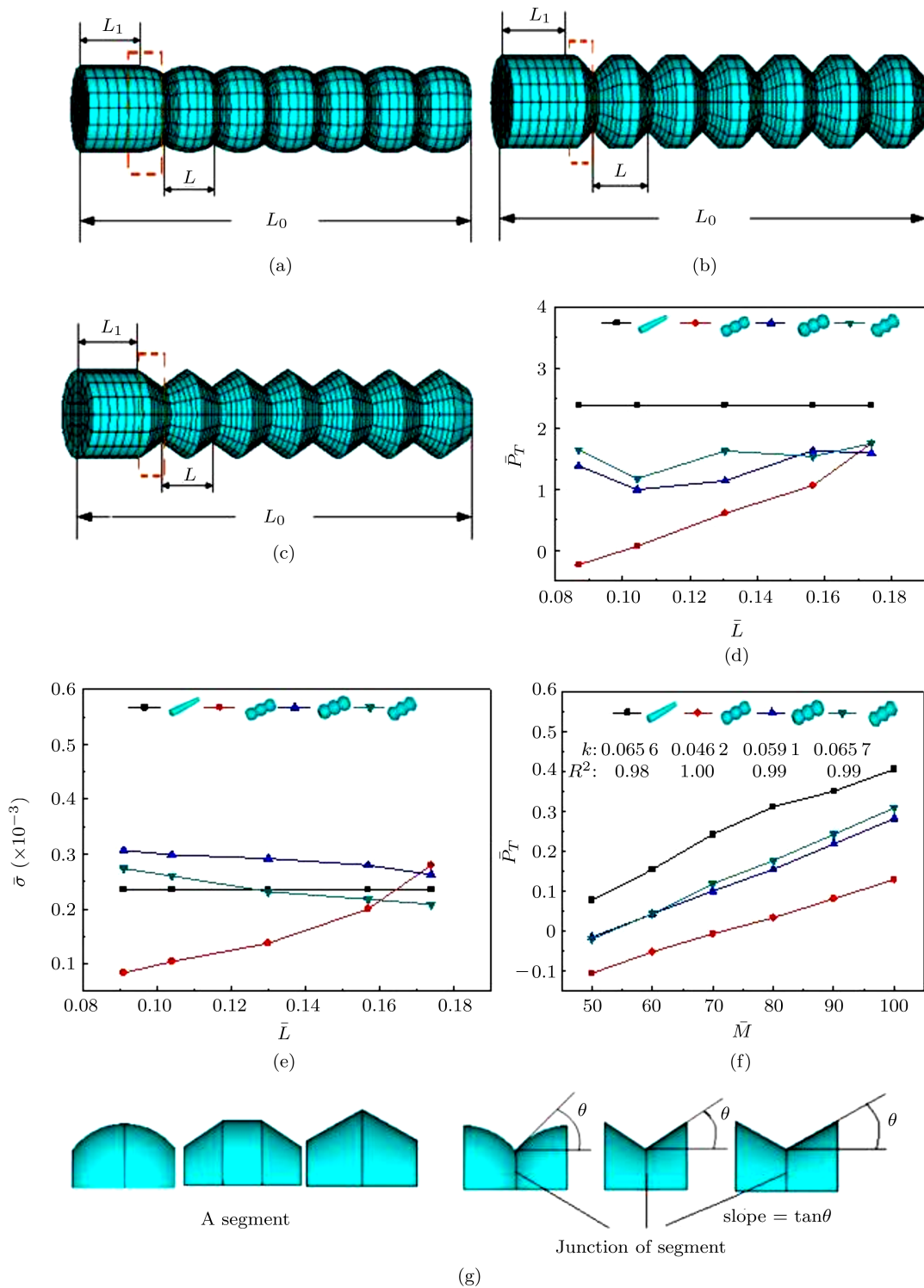


Fig. 3. Mechanical analysis of the proposed new plug structures: Schematic diagram of (a) candied gourd model; (b) thread model; (c) platform model. Comparison of (d) reactions of constraint and (e) maximum axial stress with different L ; (f) the reaction of constraint under different body weights, and (g) the segment, slope and junction of segments for different structures.

tures, i.e., candied gourd model (Fig. 3(a)), thread model (Fig. 3(b)) and platform model (Fig. 3(c)). We compared their mechanical behavior to clinically used plug model, i.e., the reactions at suture part of plug (Fig. 3(d)), the max axial stress in the plug to prevent fracture (Fig. 3(e)), and effect of body weight on reaction (Fig. 3(f)).

The parameters in Fig. 3(a)–3(f) are defined as $\bar{L} = L/L_0$, $\bar{P}_r = P_r/P_0$, $\bar{\sigma} = \sigma/\sigma_s$, $\bar{M} = m/m_0$, where L is the length of a segment. The P_r is the reaction of the axial displacement constraint on surface, σ is the maximum axial stress of a model, σ_s is the fracture limit for uniaxial tension of SIS (12 MPa),¹² m is the body weight and m_0 is the average body weight 70 kg.

To compare the mechanical behavior of different plug structure, we first checked the reactions under different \bar{L} for $\bar{M} = 1$ (Fig. 3(d)). The results show that for candied gourd model the reaction is the least when $\bar{L} = 0.1$. This is because the pressure P applied on every segment balances on axial direction. Then the resultant forces on axial direction is the sum of axial forces induced by P_0 applied on the left side of plug and the axial component of P that applied on the surface of the half segment (red dash box in Fig. 3(a)–3(c)) connecting the suture part. When \bar{L} is changed, the surface area of the half segment and its tilt angle are changed. When $\bar{L} = 0.1$, the resultant force is least for all the three new models.

For the three new models, the maximum axial stress is located at junction of segments. From the curve of candied gourd model, we found that the stress $\bar{\sigma}$ increases with increasing \bar{L} . When \bar{L} increases from 0.08 to 0.18, the slope of surface also increases from 0.43 to 1.34 (Fig. 3(g)), which makes the stress concentration effect more serious resulting in increased maximum axial stress. In the cases of thread and platform models, $\bar{\sigma}$ decreases with increasing \bar{L} . This is associated with the increase of \bar{L} from 0.08 to 0.18, the slope of surface decreases from 1.42 to 0.77 for thread model and from 1 to 0.5 for platform model (Fig. 3(g)). So the stress concentration gets less serious owing to decreased maximum axial stress. From Fig. 3(e), we found that under the physiological condition, the maximum stress (0.6–5 kPa) for all the models is far smaller than the tensile strength of SIS material (1.2 MPa). This result indicates that the mechanical loading on the plug is within

the safe range.

To checked the effect of body weight, we performed the simulation of different body weights from 50 kg to 100 kg with $\bar{L} = 0.1$ which gives smallest reaction (Fig. 3(d)). We observed a linear relationship between reaction and body weight (the slopes are 0.065 6, 0.046 2, 0.059 1, 0.065 7 for cone-shape model, candied gourd model, thread model and platform model respectively). We also observed that the reaction of constraint for candied gourd model is always smaller than other models in the range of body weight.

In summary, we developed an FEM model for fistula plug under physiological condition in this study. We also proposed three new plug structures with decreased mechanical loading on the plug compared to clinically used plug. The results of parameter analysis indicate that the candied gourd model with $\bar{L} = 0.1$ gives the smallest reaction and axial stress compared to other structures, which holds great potential to improve anal fistula plug falling.

This work was supported by the Major International (Regional) Joint Research Program of China (11120101002), the National Natural Science Foundation of China (10825210 and 31050110125) and the National 111 Project of China (B06024).

1. P. Lunniss, and M. Kamm, British Journal of Surgery **81**, 1382 (1994).
2. H. Geckil, F. Xu, and X. Zhang, et al., Nanomedicine (Lond) **5**, 469 (2010).
3. M. Whiteford, Diseases of the Colon & Rectum **48**, 1337 (2005).
4. E. Johnson, and J. Gaw, Diseases of the Colon & Rectum **49**, 371 (2006).
5. O. Schwandner, S. F. Dietl O, International Journal of Colorectal Disease **23**, 319 (2008).
6. B. Champagne, Diseases of the Colon & Rectum **49**, 1817 (2006).
7. P. Garg, Colorectal Disease **11**, 588 (2008).
8. P. van Koperen, BMC Surgery **8**, 11 (2008).
9. R. Q. Erkamp, P. Wiggins, and A. R. Skovoroda, et al., Ultrasonic Imaging **48**, 2183 (1998).
10. C. B. M. & M, A. E, Rubber Chemistry and Technology **73**, 504 (2000).
11. S. Badylak, *Tissue Engineering: Current Perspectives* (Cambridge, Burkhauser Publishers, 1993).
12. N. X. Wen, Journal of Medical Biomechanic **22**, 75 (2007).